A Wide-Band Square-Law Circuit Element

A. S. SOLTES†

Summary—**A square-law circuit element with operating frequency range from zero into the vhf region is described. Its dynamic range and accuracy capabilities vary with the particular conditions under which it is operated; accuracies within less than one per cent of full scale and output dynamic ranges of over 100 db have been achieved. Frequency response limitations and possible sources of error are analyzed. Experimentally determined characteristics are presented and noise properties, dynamic range, and accuracy potentialities evaluated.**

Introduction

THE APPLICATION of electronic techniques to high speed analog computing and automatic control has brought with it the need for circuit elements that have accurate, reproducible, prescribed mathematical characteristics and are capable of operating at the speeds afforded by conventional circuit components.

The square-law circuit element was originally developed to satisfy the need for a wide-band circuit element around which a square-law amplifier could be designed capable of operating on a continuous stream of short, pulsed carrier signals, such as might appear, for example, in a radar IF amplifier. Square-law range of 40 db at output (accuracy within one per cent of full scale) was required.

A review of existing methods for generating nonlinearities, such as the static characteristics of conventional vacuum tubes and crystals, alone or in networks,[1-4] biased diodes,[5-7] conventional square-law detectors, and feedback type function generators,[8-11] revealed that for our purposes all were either too inaccurate or had insufficient bandwidth.[12] A new approach was, therefore, necessary to develop a suitable square-law device. As a component possessing a parabolic transfer characteristic over a wide frequency range, this square-law device is potentially applicable wherever a true mathematical square-law characteristic is required.

It has been used to satisfy the requirements of the square-law amplifier application described above,[13] and has also been successfully employed in a high speed function multiplier circuit of the quarter-square type.[14] It may find other useful applications in linear modulators of the suppressed carrier type, detectors, phase meters and other computer operations such as squaring and square-rooting. The principle of operation may also be employed to generate other prescribed nonlinearities.

Description

The method chosen for obtaining the required wide-band square-law action was to deflect a sheet of electrons across suitably shaped target electrodes in a beam-deflection tube, as shown in Fig. 1. The input voltage is applied to the deflection plates, and the output current is drawn from either the shaped mask or collector electrodes, or both. The output current is thus some function of the input voltage determined by the geometry of the electron beam and the shaped target. A rectangular co-ordinate type of geometry is shown in order to simplify the description.

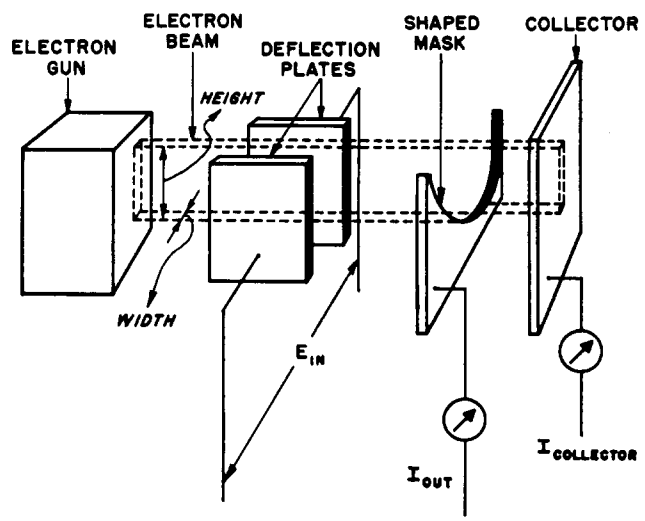

Fig. 1—Functional schematic of beam deflection tube.

This method is essentially "inertialess" and hence adaptable to a wide range of frequencies limited only by transit time. Furthermore, the same approach may be used to produce a variety of transfer characteristics by merely modifying the target shape.

† Computer Lab., Elec. Res. Directorate, AF Cambr. Res. Ctr., Cambridge, Mass.

[1] B. Chance, V. Hughes, E. F. MacNichol, D. Sayre, and F. C. William, "Waveforms," M.I.T. Radiation Lab. Ser., vol. 19, sec. 19.6, McGraw-Hill Book Co., Inc., New York, N. Y.; 1949.

[2] J. H. P. Draper and D. G. Tucker, "A square-law circuit," *Jour. Scien. Instr.*, vol. 24, pp. 257–258; October, 1947.

[3] H. McG. Ross and A. L. Shuffrey, "An electronic square-law circuit," *Jour. Scien. Instr.*, vol. 25, pp. 200–202; June, 1948.

[4] J. S. Rochefort, "A Germanium-Diode Square-Law Device," Northeastern Univ. Elec. Res. Proj., Boston, Mass.; Sept., 1951.

[5] B. Chance, J. Busser, and F. C. William, "A fast multiplying circuit," presented meeting American Physical Society, April, 1950; *Phys. Rev.*, Abstract, July, 1950.

[6] B. O. Marshall, Jr., "An analogue multiplier," *Nature*, vol. 167, pp. 29–31; January, 1951.

[7] J. J. Gait, "A High Speed Squaring and Multiplying Circuit," RAE Tech. Memo No. GW97; December, 1949.

[8] W. E. Gilson, "Medical stimulus circuits," *Electronics*, vol. 21, p. 99; July, 1948.

[9] A. B. MacNee, "An Electronic Differential Analyzer," Tech. Rep. No. 90, Res. Lab. Elec., M.I.T., Cambridge, Mass.; Dec., 1948.

[10] D. E. Sunstein, "Photo-electric waveform generator," *Electronics*, vol. 22, pp. 100–103; February, 1949.

[11] A. C. Munster, "The monoformer," *Radio-Elec. Engrg.*, vol. 15, pp. 8A–9A; October, 1950.

[12] Several of the references cited were not published when this research was started; however, the statement is still generally true.

[13] A. S. Soltes, "A wide-band square-law computing amplifier," *Trans. IRE*, vol. EC-3, No. 2, pp. 37–41; June, 1945.

[14] J. A. Miller, R. E. Scott, and A. S. Soltes, "Wide-band analog function multiplier," *Electronics*, vol. 28, pp. 160–163; February, 1955.

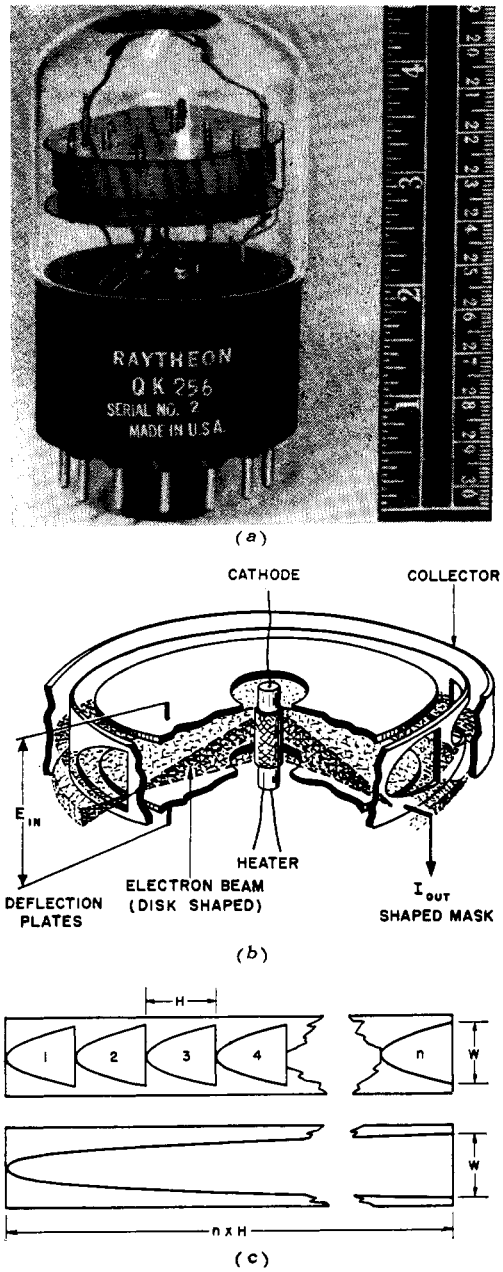

Fig. 2—(a) QK-256 beam deflection square-law tube. (b) QK-256 cut-away view. (c) Equivalent mask shapes. n short parabolas each of height "H" and width "W" are equivalent to one long parabola of height $n \times H$ and width W.

The target used to produce a square-law characteristic is parabolic in shape. As will be shown in the subsequent analysis, such a target shape is extremely tolerant with regard to the beam shape with which it must be combined to produce a square-law characteristic. Hence, although more complicated beam-forming structures are necessary to accurately produce an arbitrary transfer characteristic, an adequate design for a square-law tube may be very simple. Tubes were developed on the principle described above by the Raytheon Manufacturing Company on contract[15] with this laboratory (Raytheon Types QK-256 and QK-329). The tubes [Figs. 2(a) and (b)] have cylindrical symmetry about a cathode located on the axis of the cylinder. The gun structure is simply the cathode, and the electrons travel radially out from it in the form of a disk shaped beam. The washer-like deflection plates, located on either side of the beam, serve both to focus the electron disk on the shaped target, or mask, and to raise or lower its outer edge in accordance with the input voltage. Fig. 2(b) shows the shaped mask lying on its side in the form of a cylinder concentric with the cathode. A collector ring surrounds the target to pick up electrons not previously intercepted.

If the mask electrode were opened out flat, its shape would be a long, thin, rectangle—a difficult form within which to shape a parabola accurately. For mechanical convenience, the mask was actually divided into a number of small, identical parabolas of convenient dimensions which are the equivalent of one long parabola as shown in Fig. 2(c). This method of construction, as will be shown, also results in a reduction of distortion from certain imperfections which may occur in the fabrication of the tubes.

Frequency Response Limitations

The fundamental limitation on the frequency range of the beam deflection square-law tube is imposed by transit time. This limitation causes: (a) reduction in deflection sensitivity with increasing frequency up to transit angles of about 2π radians, and (b) above that point fluctuations in deflection sensitivity with frequency. An estimate of the potential limitation in frequency response for typical operating conditions may be made by a rough computation of the half-power frequency due to transit time. In practical units, the transit time, T, for planar electrodes is

$$T = 3.35 \times 10^{-8}\, d/V^{1/2} \text{ seconds}^{16} \qquad (1)$$

where d is electrode spacing in cm and V is the accelerating potential in practical volts.

Substituting T from (1) in (2) relating frequency, f, transit angle, Φ, and transit time

$$f = \Phi/2\pi T \qquad (2)$$

we get

$$f = 30.2 \times \Phi V^{1/2}/2\pi d \text{ mc.} \qquad (3)$$

For $d = 2$ cm and $V = 300$ v, which are typical for these tubes

$$f = 2.58 \times 10^{2}\Phi/2\pi \text{ mc.} \qquad (4)$$

It may be determined from a curve of per cent of dc sensitivity vs transit angle[17] that a reduction in sensitivity to 0.707 of that at dc corresponds to a transit angle of approximately π radians. Substituting $\Phi = \pi$,

[15] "Study of a Beam Deflection Tube Approach Toward Obtaining Nonlinear Characteristics," Reps. 1–11, Contract No. AF19 (122)-17, Raytheon Manufacturing Co., Power Tube Div.; March, 1949–January, 1952.

[16] Derived from F. E. Terman, "Radio Engineers' Handbook," McGraw-Hill Book Co., Inc., New York, N. Y., 1st ed., p. 275; 1943.

[17] G. R. Kilgore, "Beam-deflection control for amplifier tubes," *RCA Rev.*, vol. 8, p. 490; September, 1947.

$$f_{0.707} = 2.58 \times 10^2 \times 1/2 = 129 \text{ mc.} \quad (5)$$

Analysis of Properties of the Tube Structure with Respect to Possible Sources of Error in Static Characteristics

For convenience in the discussions which follow, the target structures of the tube will be assumed to be opened out flat, after the manner of Fig. 1, unless otherwise stated. The deflection axis will be referred to as the "x" co-ordinate and the $f(x)$ axis as the "y" co-ordinate.

Effect of Beam Shape

It is obvious that for the tube geometry selected, a mask shaped like the desired transfer characteristic will yield a perfect characteristic when scanned by an infinitely narrow, uniform beam. However, a practical tube has finite beamwidth and a current density distribution that approximates a Gaussian error curve; furthermore, these factors will vary with focus.

Fortunately, it turns out that if an electron sheet has uniform density, J, in the "y" dimension (i.e. $J(y)$ = const), and its density distribution in the "x" dimension, $J(x)$, does not change with deflection, it will yield a parabolic static characteristic when deflected linearly across a parabolic mask regardless of what $J(x)$ may be. This can be shown from the fact that the sum of any number of parabolas is also a parabola; that is, any polynomial of the second degree

$$y = Ax^2 + Bx + C \quad (6)$$

is a parabola. Any beam of current density cross section, $J(x)$, may be divided into a series of adjacent, infinitely narrow elements [as shown in Fig. 3(a)], each of which by itself would produce an output y_K of the parabolic form of (6) as it scanned a parabolic mask. The only difference between the outputs from different elements would be in the constants of the equation. When the output contributions of all the elements are added together, the form of the sum

$$y_1 + y_2 + y_3 \cdots + y_n = \sum_0^n y_K = \sum_0^n A_K x^2 + \sum_0^n B_K x + \sum_0^n C_K \quad (7)$$

is still a second degree polynomial and hence a parabola. The scale factor of the parabola and the location of its vertex with respect to the origin may vary as the beam cross section is changed. In general, any finite beamwidth will cause the vertex to rise above the horizontal axis, and any asymmetry in the beam will cause a horizontal translation of the curve to one side or the other of the vertical axis. However, the vertex may be made to coincide with the origin of the axes, if desired, by means of external circuitry.

In addition to insuring a static characteristic whose curved portion is uncritical, the fact that the curvature of the output current curve of the tube is independent of the beamwidth may be used to enhance the accuracy of the

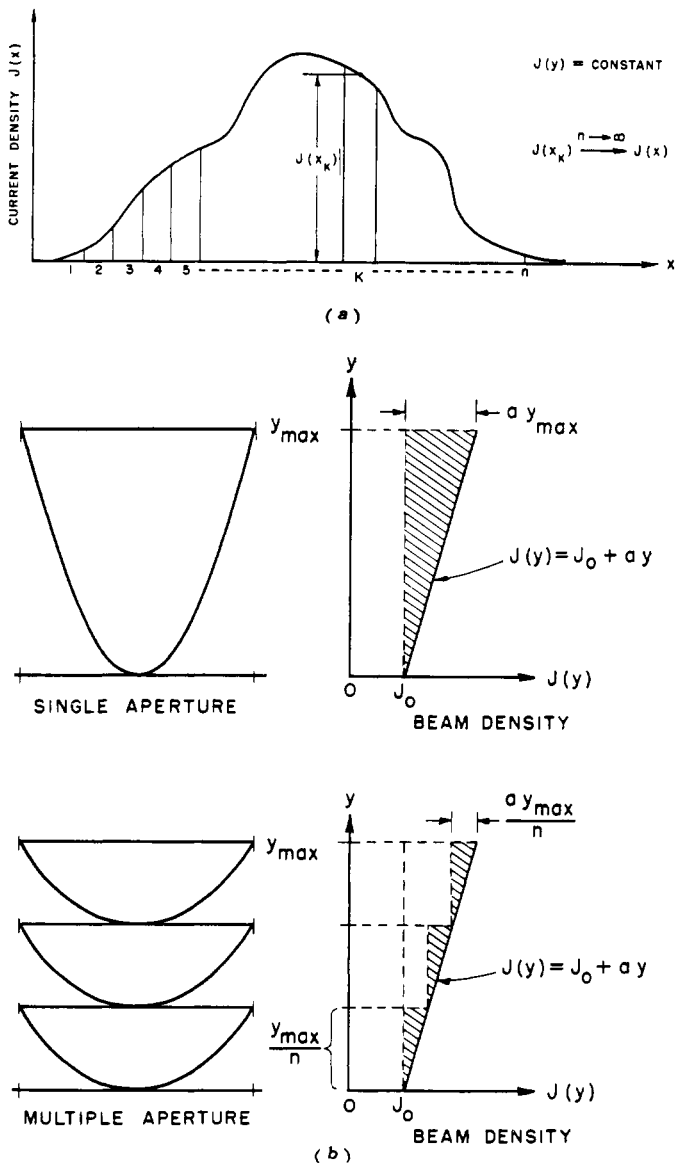

Fig. 3—(a) Analysis of cross section of current density in beam. Division of electron beam with current density cross sections $J(y)$ = constant and $J(x)$ into n adjacent, infinitely narrow elements of uniform current density $J(x_k)J(y)$. (b) Effect of multiple apertures on beam-density variations in y dimension. Shaded areas represent the effective variational portion of the beam, v. For single aperture case (top):

$$\frac{a y_{\max}^2}{2} \equiv v_1.$$

For equivalent multiple (n) apertures case (bottom):

$$\frac{a y_{\max}^2}{2n} \equiv v_n = \frac{v_1}{n}.$$

characteristic under certain conditions. If the mask has small imperfections in its contour—such as bumps or depressions—the beam may be spread so as to reduce its resolving power with respect to such variations, thus smoothing out the transfer characteristic without affecting its basic curvature.

Variations of beam current density in the "y" dimension, $J(y)$, over any aperture are an obvious source of error. The circular symmetry of the disk beam precludes edge

effects since the beam is continuous. However, variations in cathode coating for example, might cause nonuniformities. By dividing the mask into n apertures instead of one, the extent of the variation per aperture is reduced as compared to the single aperture case by a factor dependent upon n. This is shown graphically in Fig. 3(b) for a simple illustrative case in which a linear variation of $J(y)$ is assumed.

Mechanical alignment of the n apertures is not a critical factor since horizontal misalignment would not affect the curvature, although allowable deflection range would be affected and hence the magnitude of the upper limit of parabolic curvature.

Effect of Tilted Beam

Tilting of the beam away from a position parallel to the y axis of the mask will distort the output by an amount dependent upon the degree of tilt and the height of the mask aperture. In the extreme, the maximum slope of mask contour, which can be followed as a single-valued curve, will be limited by the degree of tilt.

The geometry of the tilted beam condition is shown in Fig. 4(a), an infinitely narrow beam being assumed. It can be seen that a normalized parabolic mask

$$y = x^2 + b \tag{8}$$

intercepts a portion

$$l = y_D = x_D^2 + b \tag{9}$$

of an untilted beam deflected an amount x_D, to provide a square-law output. However, when the beam is tilted away from the y-axis by an angle θ, it intersects the plane of the mask along the line

$$y = (x - x_D)/m, \tag{10}$$

where m is the tilt slope

$$m = \tan\theta = \frac{\Delta x}{y_{\max}}. \tag{11}$$

The intercepted portion of the tilted beam is then

$$l' = y_D' \sec\theta = y_D'\sqrt{1 + m^2}, \tag{12}$$

where y_D' is the intercept of (8) and (10),

$$y_D' = \frac{1 - 2mx_D - \sqrt{1 - 4m(x_D + bm)}}{2m^2}. \tag{12a}$$

Since the output current is proportional to l', the intercepted portion of the beam, l' vs x_D represents the shape of the static characteristic resulting from a parabolic mask linearly scanned by a tilted beam. (The factor sec θ may be ignored without affecting the shape of the characteristic since it is a constant for a given degree of beam tilt. Its omission normalizes the results for different amounts of beam tilt to permit easy comparison with a true square-law characteristic, so that

$$i_{\text{out}} \propto y_D'.) \tag{13}$$

The curve y_D' vs x_D is no longer square-law. It is similar to the shape of the parabolic mask rotated about its origin by an amount equal to and in a direction opposite to the beam tilt. The effect of b, which represents "land" in the mask, is to cause the apex of the curve to move off-center by an amount x_0

$$x_0 = -bm.$$

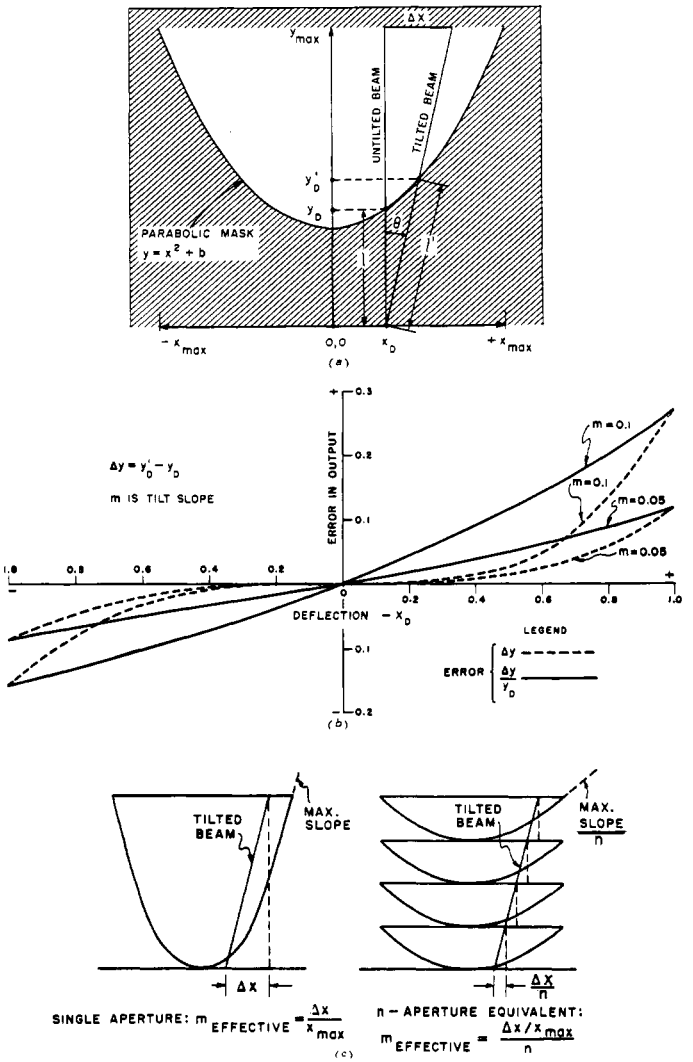

Fig. 4—(a) Geometry of the tilted beam condition. (b) Normalized errors in static characteristic arising from a tilted beam. (c) Effect of multiple apertures on beam tilt.

The normalized deviation of the curved portion of y_D' from square-law may be obtained more conveniently while assuming $b = 0$. Then the error is

$$\Delta y = y_D' - y_D = y_D' - x_D^2$$

$$= \frac{1 - 2mx_D - \sqrt{1 - 4mx_D}}{2m^2} - x_D^2, \tag{14}$$

where the variables have been normalized and are expressed as fractions of full scale values $x_{\max}$ and $y_{\max}$. The tilt slope, m, defined in (11), when so normalized reduces to the beam's x projection, Δx, divided by $x_{\max}$, its maxi-

mum excursion along the x-axis

$$m = \frac{\frac{\Delta x}{x_{max}}}{\frac{y_{max}}{y_{max}}} = \frac{\Delta x}{x_{max}}. \quad (15)$$

Normalized error, Δy, is plotted as a function of x_D in Fig. 4(b) for several values of tilt slope, m. Corresponding values of per cent error $\Delta y/y$ are also plotted. These curves show that:

1. A given reduction in tilt, m, results in more than a proportionate reduction in error Δy.
2. The per cent error, $\Delta y/y$, decreases with x_D (a reduction in x_{Dmax} will thus reduce the maximum per cent error produced by a given tilt, m).

The above properties of the error curves point the way to several means of minimizing or correcting for the error due to tilt.

The actual construction of the shaped mask with multiple parabolic apertures rather than a single one is one way of reducing the error produced by a given beam tilt. As can be seen from Fig. 4(c), the consequence of dividing the mask into n apertures is to break up the beam into n parts each with an effective tilt, m_n, of only $1/n$ of the tilt for a single equivalent aperture, m_1, i.e.

$$m_n = \frac{m_1}{n}, \quad (16)$$

where the subscripts denote the number of identical apertures into which the target electrode is divided. The error due to any beam tilt m will, therefore, be reduced more than n-fold in accordance with 1. (The fact that each of the n parts of the beam is displaced with respect to the others along the deflection axis is being ignored since, as was indicated earlier, the curvature of their sum will remain the same if their separate contributions are parabolic.)

The effect of a tilted beam on the cylindrically symmetrical tubes is actually more complicated than shown by the analysis of the rectangular case. The line of intersection of a tilted disk beam with a coaxial cylindrical mask is sinusoidal rather than straight. However, the same general considerations apply to the cylindrical tubes as to the rectangular case.

In the case of the disk beam, the tilt may be completely eliminated by means of a uniform magnetic field of the proper strength and orientation. Conversely, to prevent tilting of the beam by stray magnetic fields (including that of the earth), magnetic shielding is desirable.

Since the percentage of error is proportional to deflection of the beam, the use of signals that are as small as possible tends to minimize the error produced by tilt—that is, the smaller the signal, the greater the accuracy. The effect in producing more accurate operation is comparable to that obtained when using smaller signals, which better satisfy small-signal approximations, with so-called "linear devices."

Noise Characteristics

In its present form, the square-law tube is not intended to serve as a low-noise input stage. Its gain under most wide-band operating conditions, where load impedances are small, is much less than one; hence, any noise generated at its output will have an even larger equivalent input magnitude. With a gain of less than one, it is not suitable for applications requiring good sensitivity. The main interest in the noise properties of the tube arises in connection with their effect on the available dynamic range as a computer. Under most conditions of operation, the noise rather than accuracy of the curvature of the static characteristic has been found to set the lower limit of the dynamic range.

In view of the nonlinear transfer characteristic of the square-law tube, conventional criteria and methods for describing and evaluating noise characteristics which assume linearity are not applicable. For example, the equivalent resistance as normally defined would be found to be dimensionally a function of bandwidth. Nevertheless, the noise properties of usual interest may easily be determined for the tube for any particular given set of conditions.

Since the "gain" of the tube is so small (the maximum "transconductance" is in the order of only a few tens of micromhos),[18] the noise at the output may be approximated reasonably well solely by the shot noise contributed by the tube operating as a diode whose plate is the output electrode. The well-known expressions for the noise currents of temperature- and space-charge-limited diodes are, therefore, applicable:

$$i_T^2 = 3.18 \times 10^{-19} I \Delta f$$

for the temperature-limited case,[19] (17)

and

$$i_s^2 = 0.67\, i_t^2 = 2.13 \times 10^{-19} I \Delta f$$

for the space-charge-limited case, [19] (18)

where I is the plate current, Δf is the bandwidth and i_T and i_s are the temperature- and space-charge-limited noise currents, respectively.

The equivalent noise voltages at input or output may be determined from these equations. For example, the equivalent input noise voltage of the tube operated under space-charge-limited conditions is:

$$e_{in} = (i_s/k)^{1/2} = 2.15 \times 10^{-5}(I\Delta f)^{1/4}/k^{1/2}, \quad (19)$$

where I = average current; Δf = bandwidth.

For the QK-329 operating at $B+ = 150$ volts,

$$k = 2 \times 10^{-7} \quad \text{and} \quad I = 5 \times 10^{-4}.$$

[18] "Transconductance," $\Delta i_{out}/\Delta e_{in}$, for a square-law device $i_{out} = ke_{in}^2$ is

$$\frac{\Delta i_{out}}{\Delta e_{in}} = 2ke_{in},$$

so that it is a maximum when $e_{in} = |e_{in}|_{max}$.

[19] Terman, *op. cit.*, p. 293.

Thus, for example, for $\Delta f = 5$ mc,

$$e_{in} = 0.347 \text{ volts.} \tag{20}$$

If improvement of the noise properties of such tubes were desired, it is evident from (19) that increases in k would produce the strongest reductions in equivalent input noise. However, no net gain in dynamic range would be achieved in this manner for a given available total current, since the resulting equivalent input noise reduction would then be accompanied by a corresponding reduction in maximum input level.

Reducing I of (19) by decreasing output current at zero input signal, does offer a means of reducing output noise current so that an increase in dynamic range could be effected. In order to minimize the zero signal current, (a) the target electrode should have as little land [b of (8)] as possible, and (b) the beam should be as narrow as possible in the plane of the target.

Experimentally Determined Static Characteristics, Dynamic Range, and Accuracy Capabilities

A series of developmental beam-deflection tubes of increasing complexity were all designated QK-256 by Raytheon Manufacturing Company, Waltham, Mass.; serial numbers were used to identify the different models. QK-256, serial no. 2, proved to be adequate for our applications, and had the further advantages of simple design and power requirements. Subsequent copies of this particular model, with minor modifications, were designated QK-329. Most of the experimental data included in this Section was obtained with either the QK-329, or its prototype, and should be considered as representative rather than comprehensive. Table I gives operating parameters and characteristics typical of this tube. With more complicated tube designs in the QK-256 series, higher output currents with lower input signal requirements were achieved. Other variations which would reduce interelectrode capacitances are also possible.

TABLE I
QK-329 Data

General Characteristics	
Heater	
Voltage	6.3 volts
Current	0.6 amperes
Input Capacitance (approx.)	3 $\mu\mu$f
Output Capacitance (target)	13 $\mu\mu$f
Direct Interelectrode Capacitance (approx.)	
Between Deflector Plates	1 $\mu\mu$f
Between each Deflector Plate and Target	2.5 $\mu\mu$f
Between each Deflector Plate and Cathode	1.5 $\mu\mu$f
Between Target and Collector	8 $\mu\mu$f
Typical Operation	
Deflector Plates	+80 volts
Target	+300 volts
Collector	+300 volts
Cathode current	10 ma
Target Load Resistance	100,000 ohms
Input Signal (between deflector plates)	65 volts (peak)
Deflector Current Max (through 10,000 ohm resistance)	10 μA
Square-law voltage output*	55 volts (peak)

* The portion of the output voltage, measured from the minimum point, that is square-law within 3 per cent.

Static Characteristics

Once suitable operating conditions were determined, the expected insensitivity of the square-law curvature of the static characteristics to other parameters of a beam-deflection tube was borne out by the experimental work.

It was found that satisfactory and stable operation could be obtained by biasing the deflection plates at some constant fraction of the high voltage or E_{B+} supply. This supply voltage could then be varied over wide limits with little change in the curvature of the static characteristics, except for the location of the overload point, as is shown in the typical curves of Figs. 5(a) and 5(b) on the next page, that were obtained with an oscilloscope.

As determined by more precise means [see Fig. 5(c) next page], these curves are naturally square-law within less than one per cent of full scale over a considerable portion of the total range say, $e_{in} \leq \pm 40$ volts. The geometry of the tube makes it possible to obtain such results without careful adjustment of the operating conditions. For most purposes, then, the static characteristics, i_{out} vs e_{in}, can be idealized and described as parabolas with their vertexes displayed from the origin by amounts i_0 and e_0 so that

$$i_{out} = i_0 + k(e_0 + e_{in})^2 \quad \text{amps,} \tag{21}$$

where k is the scale factor of the parabola expressed in mhos/volt.[20] i_0 and e_0 may be functions of $B+$, beam-density cross section, alignment, aging, etc., but k and the parabolic curvature are essentially constant for a particular tube under the operating conditions described. The magnitude of k for tubes such as the QK-256 no. 2 and QK-329 with the simple (but relatively insensitive) gun structure shown in Fig. 2 is around 0.2 micromhos/volt. Values of k of the order of 10 micromhos/volt have been achieved with more complicated gun structures.

Dynamic Range and Accuracy Capabilities

For those circumstances where a high order of accuracy or dynamic range is required, more detailed information on the practical limits to the square-law behavior provided by the tube geometry is essential. Deviations of actual static characteristics from the idealized form of (21) show up when the input signal reaches a sufficiently high level, and occur in either of two forms.

Overload: A gradual but progressive falling off of the output current from the true square-law curve occurs with increasing input signal until a maximum is reached beyond which the output remains constant or decreases with further increase in input signal. This effect is equiv-

[20] The term "transquaductance" for k has been suggested by W. H. Huggins of this Center.

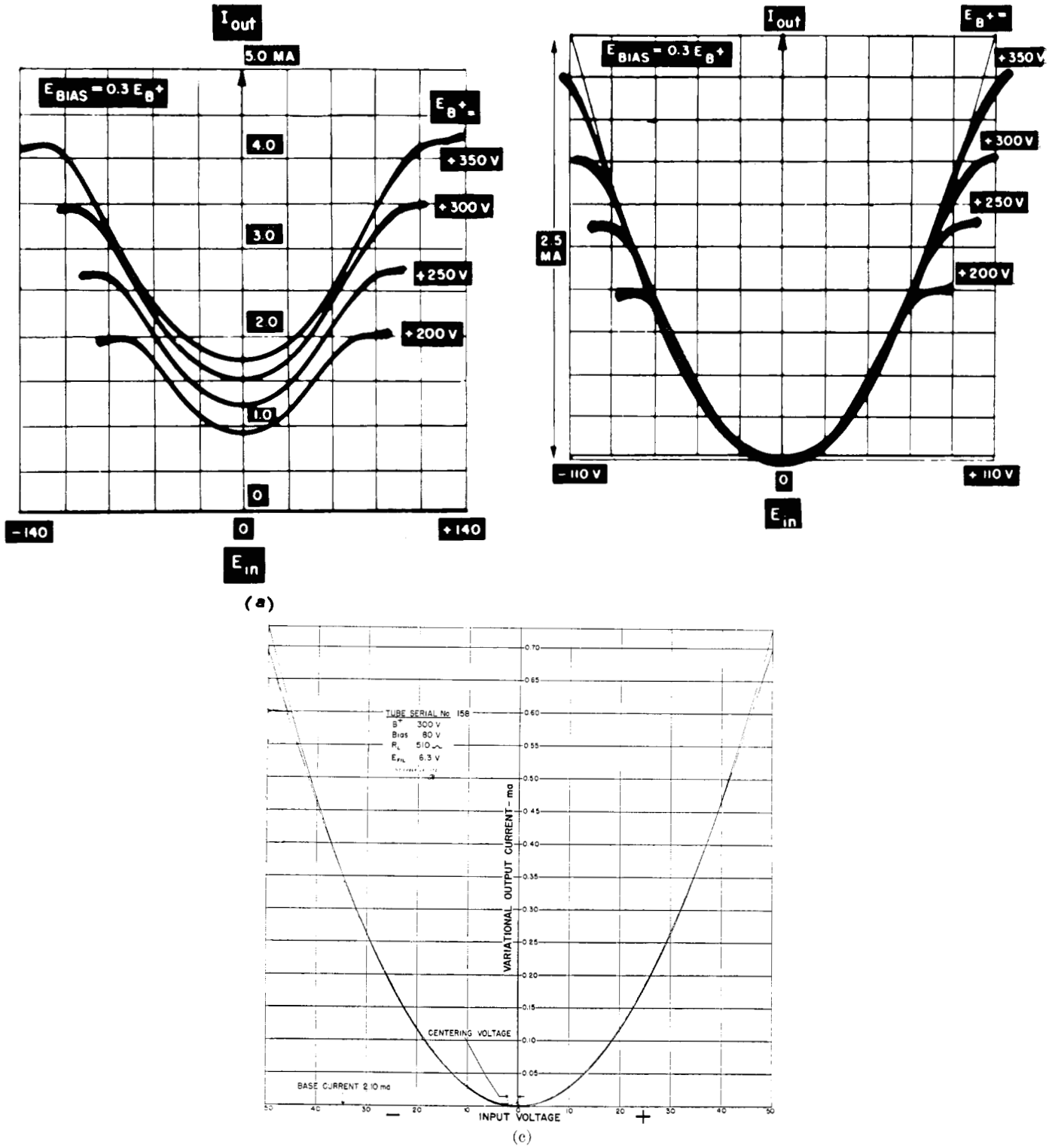

Fig. 5—(a) Static characteristics of QK-256, serial no. 2. (b) Comparison of curved portions of (a) with parabola. (c) Precise plot of static characteristic of QK-329 compared with parabola.

alent to overload in a conventional tube and imposes the ultimate upper limit to the dynamic range under any condition of operation. The manner in which this overload occurs—such as the input level at which it begins and the rate at which it progresses with further increase in input voltage—will vary with the operating conditions. Bearing in mind that the overloading is caused simply by deflection of portions of the electron beam beyond the limits of the aperture in the target electrode, it is apparent that sharply-focused beams will allow the largest undistorted deflections with accompanying abrupt overloading. On the other hand, broadly-focused beams will produce gradual overload commencing at smaller values of deflection. The absolute magnitudes of input voltage and output current at which overload takes place will be subject to additional factors that affect the total current

or the deflection sensitivity, such as $B+$. As may be seen from Fig. 5(b), the output current range from minimum current to overload point increases with $B+$. In order to achieve higher output current ranges, $B+$ might be profitably increased until the tube current becomes limited by emission saturation.

Beam Tilt: A progressive asymmetry between the two arms of the parabolic static characteristics may be evident with increasing input level, because the beam may not be parallel to the y-axis of the target. (This effect is distinct in origin from asymmetry produced by overloading with an asymmetrical electron beam.) As described heretofore (*"Effect of Tilted Beam"*), this distortion may be minimized by proper tube design and construction or completely eliminated by external means. Since the overload form of distortion is inevitable under any condition, for practical purposes the beam-tilt error need be minimized only to the point where it is overshadowed by the error from overload.

Measurements have confirmed that the lower end of the dynamic range is bounded by tube noise rather than incorrect curvature of the characteristic. Since this noise is a function of circuit bandwidth and tube current, the ultimate dynamic range will be a function of bandwidth and any factors that affect the tube current, such as high voltage supply. It was pointed out above that this supply voltage also affects the upper limit of the dynamic range—that imposed by overload. As $B+$ is increased then, the upper limit of the dynamic range, set by overload, will increase in direct proportion to any accompanying rise in total current, while the lower limit, set by noise, will rise as the square-root of this same tube current. A net gain in dynamic range may be expected, therefore, from an increase in supply voltage because of the accompanying increase in total current, until emission saturation of the tube current becomes a limiting factor.

It may be possible to obtain better performance for particular applications by taking advantage of the flexibility of operation afforded by the tube itself. It lends itself to use with a balanced or a single-ended input; single-ended output from target or collector, or push-pull output from both; and with numerous combinations of electrode potentials and loads. Particular applications may also permit operation of the square-law tube circuitwise so as to make the accuracy independent of certain factors, with resultant increase in accuracy and/or decrease in circuit complexity. For instance, if conditions allow selection of only the second harmonic component of the total output from the tube as the desired signal, its square-law action will be independent of the i_0 and e_0 terms of (21). This may be shown by substituting $e_{in} = E \cos \theta$ into (21), in which case the coefficient of the $\cos 2\theta$ term is $kE^2/2$. If the static characteristic of the tube is represented by a power series, the second harmonic component of the output can be shown to be independent of the odd order coefficients of the series for a perfectly centered input signal. Over 100 db of accurate output dynamic range has been measured using a narrow-band, second harmonic amplifier circuit and the moderately high value of $E_{B+} = 400$ volts with noise setting the lower limit.[21] For convenience these measurements were performed at audio frequencies.

Zero Stability

Applications involving dc-coupling of the square-law tubes require that the location of the vertex of the parabola with respect to the origin (i_0 and e_0 of (21)) remain constant with time, so that variations in i_{out} will be produced only by changes in e_{in}. A complete investigation of the drift characteristics of i_0 and e_0 and methods for optimizing their stability has not yet been concluded. However, preliminary results indicate that input drift is negligible; e_0 may vary from tube to tube but remains at the same value for a given tube without critical adjustment of tube potentials. Self-zeroing schemes at the input are unnecessary. Output current and i_0, however, being functions of total current, are sensitive to any parameters that affect total current, such as filament voltage and E_{B+}. The normal precautions appropriate to dc-amplifier design must, therefore, be taken to hold i_0 stable with time. These conclusions are indicated qualitatively by the static characteristics of Fig. 5(a).

Conclusion

Beam deflection square-law tubes have been developed which provide accurate static characteristics with inherent parabolic curvature usable over a frequency range from zero into the vhf region.

Dynamic range is bounded by overload at the high end and noise at the low end. Dynamic range and accuracy capabalities are dependent upon the particular operating conditions. Accuracies within less than 1 per cent of full scale and output dynamic ranges of over 100 db have been achieved. Successful applications to date give promise for much wider application in the future.

Acknowledgment

Full credit for the design and construction of the beam deflection tubes described herein is given to B. C. Gardner[22] and R. M. Unger of the Raytheon Manufacturing Company. The precise static characteristic [Fig. 5(c)] was obtained by A. Moccia and H. Brun of the Electronics Research Directorate, AF Cambridge Research Center.

[21] W. T. Rusch, "Dynamic Range Measurements of Square-Law Tube QK-329 at Audio," AF Cambr. Res. Ctr. Rep. No. E-4091; December, 1952.

[22] Now with Varian Associates, Palo Alto, Calif.